Makara Journal of Science

Volume 26
Issue 3 *September*

Article 4

9-30-2022

Synthesis of Alginate/Hydroxyapatite Beads for Acetaminophen Delivery

Anesylvia Angan
Department of Chemical Engineering, Universiti Teknologi PETRONAS, Perak 32610, Malaysia

Nonni Soraya Sambudi
Department of Chemical Engineering, Universitas Pertamina, Jakarta Selatan 12220, Indonesia, nonni.ss@universitaspertamina.ac.id

Recommended Citation

Angan, Anesylvia and Sambudi, Nonni Soraya (2022) "Synthesis of Alginate/Hydroxyapatite Beads for Acetaminophen Delivery," *Makara Journal of Science*: Vol. 26: Iss. 3, Article 4.
DOI: 10.7454/mss.v26i3.1385
Available at: https://scholarhub.ui.ac.id/science/vol26/iss3/4

Makara Journal of Science, 26/3 (2022), 182–189
doi: 10.7454/mss.v26i3.1385

Synthesis of Alginate/Hydroxyapatite Beads for Acetaminophen Delivery

Anesylvia Angan[1] and Nonni Soraya Sambudi[2*]

1. Department of Chemical Engineering, Universiti Teknologi PETRONAS, Perak 32610, Malaysia
2. Department of Chemical Engineering, Universitas Pertamina, Jakarta Selatan 12220, Indonesia

[*]*E-mail: nonni.ss@universitaspertamina.ac.id*

Received July 13, 2022 | Accepted September 12, 2022

Abstract

Conventional drug delivery systems usually involve the intake of multiple drugs, which could amplify the risk of overdosing. Acetaminophen is a widely used pain relief substance that is prone to accidental overdosing. Hence, a controlled drug delivery system is needed to ensure its efficacy. A nanocomposite hydroxyapatite/alginate system that was used as a drug carrier for acetaminophen was synthesized through the sol-gel method, and the mechanism underlying its controlled drug delivery was investigated. Spherical nanocomposite bead samples were synthesized by incorporating 5 wt%, 10 wt%, and 15 wt% hydroxyapatite into mixtures containing alginate. The mixtures were then dropped into calcium chloride solution. The phase purity of the hydroxyapatite sample was confirmed through X-ray diffraction, and the functional groups that confirmed the presence of alginate and hydroxyapatite in the nanocomposite samples were analyzed by using Fourier transform infrared spectroscopy. The release of acetaminophen can be controlled for 48 h, and the Korsmeyer–Peppas kinetics model showed the best correlation for all samples. The kinetics of Al/HAp5, Al/HAp10, and Al/HAp15 were governed by quasi-Fickian diffusion with the n values of 0.199, 0.238, and 0.225, respectively. The composite beads show potential for application as a controlled drug delivery vehicle.

Keywords: acetaminophen, alginate, diffusion, hydroxyapatite, release

Introduction

Traditionally, the administration of medical drugs to gain therapeutic benefits is done by consuming these drugs through several routes, such as inhalation, and oral and transdermal administration. However, despite having been proven to be successful in delivering pharmacological substances, conventional drug delivery systems still have drawbacks in controlling the rate of drug delivery to the targeted site [1]. Conventional drug delivery systems are associated with the high likelihood of drug overdose due to repeated and voluntarily drug consumption. Moreover, the distribution of unnecessarily high doses to nontargeted body cells and tissues may result in serious adverse effects during treatment [2]. One of the commonly consumed drugs for treatment is acetaminophen, which is used as an analgesic and anti-inflammatory treatment for headaches, colds, or common pain. The U.S. Food and Drug Administration reported that acetaminophen overdose has become the most common cause of liver transplantation, with 50% of cases caused by accidental overdosing [3]. Therefore, the development of drug delivery technologies is needed to overcome the setbacks of conventional drug delivery. Controlled drug delivery systems are effective in ensuring high therapeutic effects and reducing the side effects of the drugs based on their ability to target specific sites only [4].

Often, in controlled drug delivery systems, an inorganic material, such as hydroxyapatite, is used as the drug carrier through electrostatic interaction and hydrogen bonding. Hydroxyapatite is a naturally occurring calcium phosphate mineral and is widely known as the main component of bone [5]. The attractive properties possessed by hydroxyapatite for utilization as a drug delivery vehicle are low solubility at physiological pH, porosity, and porous structure that can absorb high amounts of therapeutic substances and maintain sustained release [5]. Hydroxyapatite can undergo surface electrostatic and hydrophobic interactions with drug molecules [5]. Hence, increasing the loading of hydroxyapatite prolongs drug release due to the availability of additional active sites that could improve electrostatic and hydrophobic interactions [6]. Meanwhile, alginate, which is usually derived from brown seaweed, is known as a biocompatible, biodegradable, nontoxic, versatile material that can be shaped into various scaffolds to enhance cell differentiation [7]. Biopolymers, such as alginate, usually exhibit a mucoadhesive property that is advantageous for extending the contact time of therapeutic substances with the mucous

layer in the gastrointestinal track, thus prolonging and sustaining substance release [8]. The combination of alginate and hydroxyapatite has been used as a drug delivery vehicle for ciprofloxacin [9], gentamicin [10], amoxicillin [11], doxorubicin [12, 13], tetracycline hydrochloride [14], chlorhexidine [15], propranolol [16], and cloxacillin [16]. Acetaminophen is widely used as the first-line treatment of mild to chronic or persistent pain. It is usually taken multiple times a day (every 4—6 h) and is immediately released [17]. Hence, the sustained release of acetaminophen improves convenience and compliance among patients and enhances pain relief [17, 18]. The combination of hybrid organic–inorganic systems for drug delivery has provided a multipurpose system that offers advantages, such as improved drug retention, controlled release for targeted therapeutic strategy, and superior pharmacokinetics properties [19]. Given that the combination of alginate and hydroxyapatite has not been applied for the delivery of acetaminophen, this study aims to reveal the performance of this composite in the controlled release of acetaminophen and the kinetics model that fits the release profile of acetaminophen.

Methods

Materials. Calcium nitrate tetrahydrate ($Ca[NO_3]_2{\cdot}4H_2O$), diammonium hydrogen phosphate ($[NH_4]_2HPO_4$), sodium hydroxide (NaOH), and acetaminophen were purchased from Sigma Aldrich. Hydrochloric acid (HCl, 37%) was purchased from Merck. Phosphate-buffered saline (PBS), calcium chloride ($CaCl_2$), and sodium alginate were purchased from Fisher International. Deionized water was used for preparing solutions and washing. All chemicals were used as purchased without further purification.

Synthesis of hydroxyapatite. Hydroxyapatite was prepared with $Ca(NO_3)_2{\cdot}4H_2O$ dissolved in 50 ml of 0.4 M HCl solution and $(NH_4)_2HPO_4$ dissolved in 500 ml of 0.7 M NaOH solution. The Ca/P ratio was set as 1.67. At room temperature, $(NH_4)_2HPO_4$ was added dropwise into the $Ca(NO_3)_2{\cdot}4H_2O$ solution. The resulting sol was then filtered by using vacuum filtration and repeatedly washed with deionized water three times. The precipitate was collected by drying the sol in the oven overnight at 100 °C. The dried particles were then grounded into a fine powder by using a mortar and pestle.

Synthesis of hydroxyapatite–alginate beads. Bead-shaped adsorbents were prepared by following a method from a previous study with some modifications [20]. First, approximately 5 wt% hydroxyapatite was mixed with 1 wt% sodium alginate solution. Mixing was repeated with 10 wt% and 15 wt% hydroxyapatite. By using a syringe, the mixture was then dropped into the $CaCl_2$ solution at the concentration of 10 g/L. The beads from the solution were filtered and dried in an oven at 40 °C for 5 h.

Characterization of the synthesized material. The phase purity and structure of hydroxyapatite were analyzed by using an X-ray diffractometer (XRD, Bruker D8 Advance) on an X'Pert3 Powder & Empyrean PANalytical system with Cu Kα irradiation ($\lambda = 1.54$), diffraction angles (2θ) ranging from 10° to 80°, the step size of 1°/step, and the exposure time of 1 s/step. The functional groups present on the surfaces of the hydroxyapatite and beads were analyzed by using Fourier transform infrared (FTIR, Perkin Elmer) spectroscopy over the wavenumber range of 500–4000 cm^{-1}.

Acetaminophen loading and release test. Acetaminophen was dispersed into the mixture of hydroxyapatite and sodium alginate at the concentration of 20 ppm. By using a syringe, the mixture containing acetaminophen was dropped into $CaCl_2$ at the concentration of 10 g/L. The resulting beads from the mixture were then filtered through vacuum filtration and washed three times with deionized water. The beads were filtered and dried in an oven at 40 °C for 5 h. The products prepared with 5 wt%, 10 wt%, and 15 wt% hydroxyapatite were designated as Al/HAp5, Al/HAp10, and Al/HAp15, respectively. The dried beads were then used for the release test. The remaining acetaminophen solution was then analyzed by using a UV–Vis spectrophotometer (Shimadzu UV–1800) to determine the amount of acetaminophen loaded in the composite beads.

Al/HAp5, Al/HAp10, and Al/HAp15 were added into 25 mL of PBS separately. The three mixtures were then shaken at the speed of 250 rpm by using an orbital shaker with the temperature kept at 37 °C. Approximately 3 mL of the solution was taken periodically over 2 days to check for absorbance by using a UV–Vis spectrophotometer (Shimadzu UV–1800) at the wavelength of 243 nm. The sample solution was taken at the following time points: 15 min, 30 min, 1 h, 2 h, 4 h, 8 h, 24 h, and 48 h. Every 3 mL of sample taken was replaced with the same amount of fresh PBS. Cumulative drug release (CDR) was then calculated by using the formula

$$CDR(\%) = \frac{Concentration\ of\ Acetaminophen\ at\ time,t}{Maximum\ loading\ content} \times 100\%.$$

The graph of CDR against time was plotted. The curves of the graph were fitted to several kinetics models for analyzing the drug release mechanism.

Kinetics analysis. The drug release kinetics based on the zero-order kinetics model was analyzed by using Equation (1) [21]:

$$C_t = C_0 + K_0 t, \tag{1}$$

where C_t is the concentration of the drug remaining at time t, C_0 is the initial concentration of the drug, and K_0 is the zero-order rate constant. The drug release kinetics

for the first-order kinetics model was analyzed by using Equation (2) [21]:

$$\log C_t = \log C_o - \frac{K_1 t}{2.303}, \quad (2)$$

in which K_1 is the first-order rate constant. Drug release kinetics for the Higuchi kinetics model was analyzed on the basis of Equation (3) [21]:

$$Q = K_H \times t^{\frac{1}{2}}, \quad (3)$$

where Q is the cumulative amount of drug released, and K_H is the Higuchi dissolution constant. The drug release kinetics based on the Hixson–Crowell kinetics model was analyzed by using Equation (4) [21]:

$$C_o^{1/3} - C_t^{\frac{1}{3}} = K_{HC} t, \quad (4)$$

where K_{HC} is the Hixson–Crowell rate constant. The drug release kinetics based on the Korsmeyer–Peppas kinetics model was analyzed by using Equation (5) [21]:

$$M_t / M_\alpha = k.t^n. \quad (5)$$

in which M_t/M_α is the fraction of the drug released at time t, k is the rate constant, and n is the release exponent indicating the drug transport mechanism through the polymer.

Results and Discussion

Morphology. The hydroxyapatite powder (Figure 1a) was synthesized through the sol-gel method, which is also known as wet chemical precipitation. The selected method has been proven to be advantageous in achieving high-purity nanoparticles at low temperatures and ambient pressures [22]. It involves the chemical transformation of the colloidal suspension of particles, namely, sol, followed by gelation to form a gel [23]. In the synthesis of the alginate–hydroxyapatite composite, the sol-gel transition occurred immediately after the mixture of alginate–hydroxyapatite was dropped into the $CaCl_2$ solution to produce beads.

The average diameters of the Al/HAp5, Al/HAp10, and Al/HAp15 beads after synthesis were 2–3, 2–3.5, and 3.5–4 mm, respectively (Figure 1b–d). Evidently, the bead size of Al/HAp15 was slightly larger than that of the other composite beads. During the sol-gel transition, Ca^{2+} ions penetrated the alginate and interacted with PO_4^{3-} [24]. The hydroxyapatite particles then grew slowly among the alginate polymer chains [24]. The swelling of these beads was mostly influenced by the interaction among hydroxyapatite, alginate, and acetaminophen particles, as well as the amount of each component added into the mixture. Hence, the particle diameter slightly increased with the increase in the weight of the mixture.

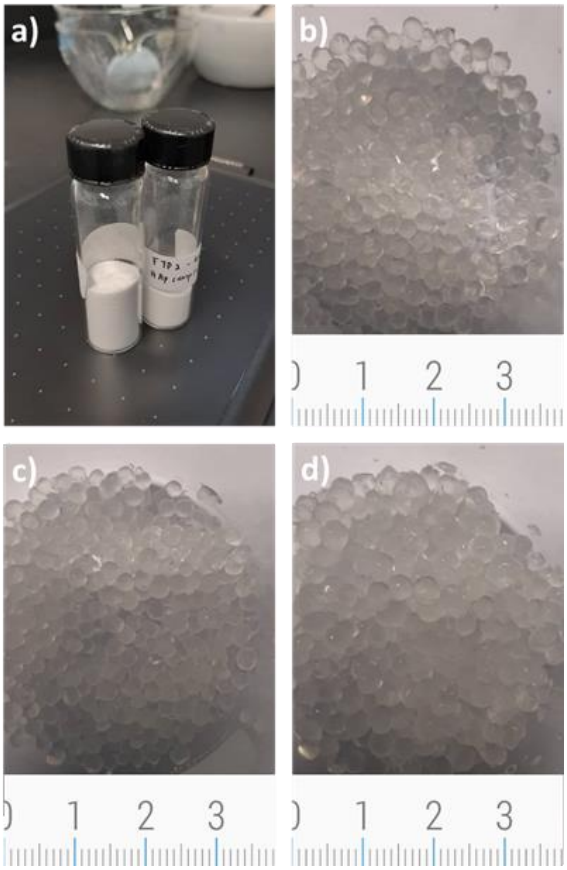

Figure 1. Measurements of a) Synthesized Hydroxyapatite, b) Al/HAp5, c) Al/HAp10, and d) Al/HAp–15 Beads. The Measurements Were Taken by using a Ruler in Units of cm.

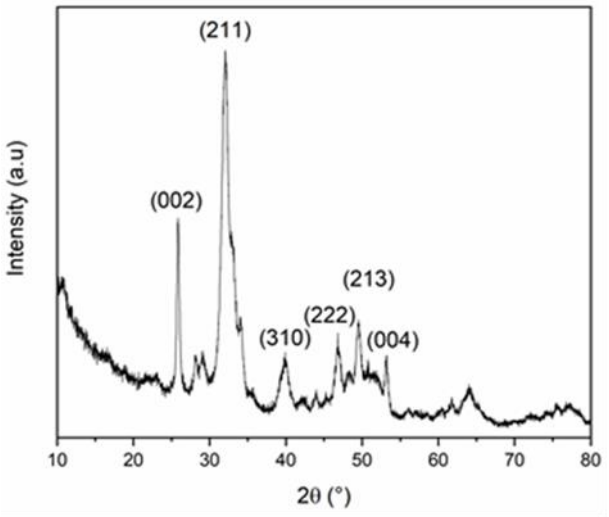

Figure 2. XRD Spectrum of the Synthesized Hydroxyapatite

Crystallinity and functional groups. The phase purity of hydroxyapatite was analyzed by using an XRD Xpert–3 system. The hydroxyapatite phase was identified on the basis of the measurement of the diffracted beam intensities at their respective diffraction angles. The diffraction patterns contained peaks at 2θ 25.87°, 32.07°, 39.92°, 46.83°, 49.53°, and 53.21° that corresponded to the diffraction planes of (002), (211), (310), (222), (213), and (004), respectively (Figure 2) [23, 25], based on the standard data for hydroxyapatite diffraction peaks provided in JCPDS 09–0432. The appearance of these prominent sharp peaks confirmed the presence of pure crystalline hydroxyapatite, $Ca_{10}(PO_4)_6(OH)_2$, as a single phase with a hexagonal structure.

The FTIR spectra of hydroxyapatite, Al/HAp5, Al/HAp10, and Al/HAp15 are shown in Figure 3a. The wide absorption peaks at 3262–3267 cm^{-1} for all Al/HAp samples were due to the stretching vibrations of O–H bonds in the presence of alginate. The band at 1605 cm^{-1} was assigned to the asymmetric C=O stretching of alginate [26]. The absorption peak at 1408 cm^{-1} can be assigned to the symmetric stretching vibration of carboxylate anions (COO^-) [27]. The band at 1326 cm^{-1} corresponded to C–O stretching vibration [28]. The absorption at peak 1082 cm^{-1} corresponded to C–O stretching vibrations (C–O–C) [9]. The overlapping absorbance peaks of hydroxyapatite and alginate at 1020 cm^{-1} can be assigned to the phosphate group(PO_4^{3-}) of hydroxyapatite [23] and C–O–C asymmetric stretching in alginate [27] (Figure 3b). The intensity of the peak at 1020 cm^{-1} slightly increased due to the addition of hydroxyapatite in the beads and can confirm the increased loading of hydroxyapatite in the beads (Figure 3b). Hydroxyapatite and alginate could interact through Ca–OH groups on the apatite surface [29]. All peaks correlated with alginate appeared in the spectra of Al/Hap. Hence, no chemical change occurred during the fabrication of the composite.

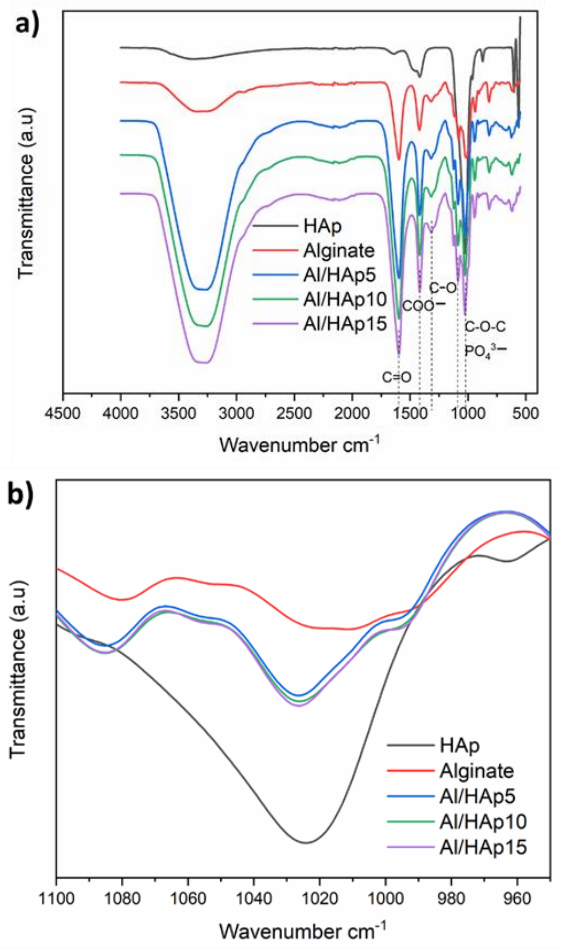

Figure 3. a) FTIR Spectra and b) Enlarged FTIR Spectra of Alginate, Hydroxyapatite, and Al/HAp Samples

Drug release and kinetics. In this experiment, acetaminophen was loaded during bead synthesis to maximize drug loading. The loading amounts of acetaminophen in Al/Hap5, Al/Hap10, and Al/Hap15 were 76.3%, 86.5%, and 90.2%, respectively. The increased loading of hydroxyapatite provided additional sites for the adsorption of acetaminophen [30, 31]. Figure 4 shows the cumulative acetaminophen release from the synthesized beads. Acetaminophen release increased in parallel with its respective absorbance with the prolongation of the release time. The CDR data showed that Al/HAp5 took only 2 h to release 51.10% of acetaminophen, whereas Al/HAp10 and Al/HAp15 took 8 and 4 h to release 53.57% and 50.76% of acetaminophen, respectively. Moreover, the early-stage release of acetaminophen from Al/HAp5 occurred at a more rapid rate than that from Al/HAp10 and Al/HAp15. The incorporation of hydroxyapatite provided additional available actives sites for electrostatic and hydrophobic interactions in the alginate matrix that helped retain

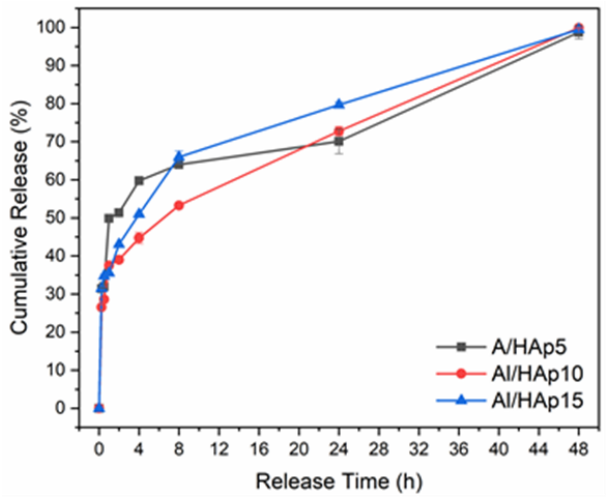

Figure 4. Profile of Acetaminophen Release from Al/HAp Samples

acetaminophen [5]. Hence, as can be deduced from the release profile, HAp-Alg-AC–10 was the optimal nanocomposite for acetaminophen release because it exhibited the most controlled, sustained, and slow acetaminophen release. Meanwhile, the excessive addition of hydroxyapatite might cause the formation of additional microchannels in the composites and thus hastened the release of acetaminophen [24]. Chen *et al*. found similar results for the loading and release of alendronate from composite hydroxyapatite microspheres [30]. The increased loading of hydroxyapatite provided additional active sites for increased drug adsorption; as a result, sustained drug release by the microspheres with hydroxyapatite was nearly five times higher than that from the microspheres without hydroxyapatite loading [30]. Pradid *et al*. improved the clindamycin loading and nontoxicity toward human lung fibroblast cells of PLA/hydroxyapatite microspheres by increasing the amount of hydroxyapatite in the composites [31].

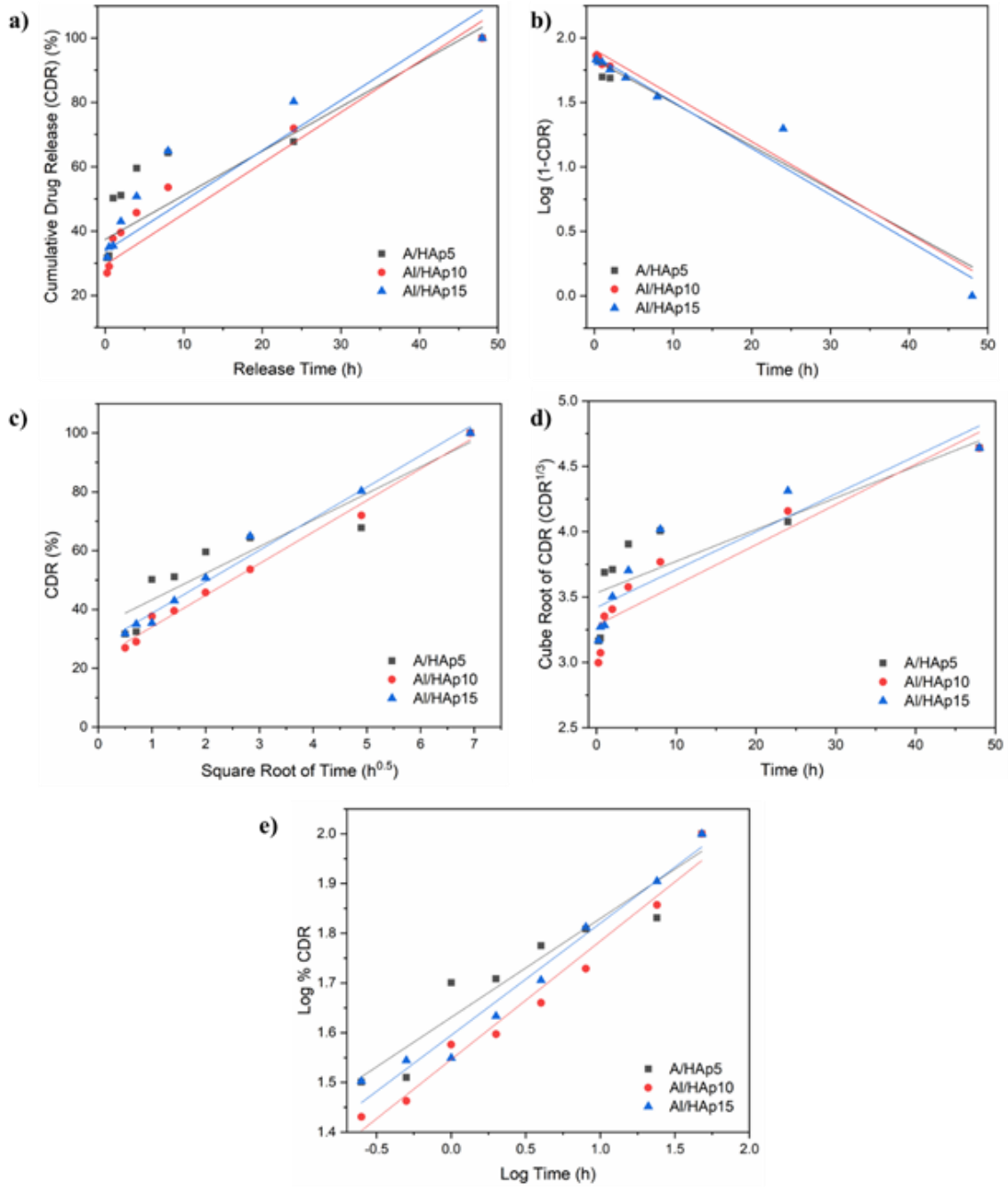

Figure 5. a) Zero-order, b) First-order, c) Higuchi, d) Hixson–Crowell, and e) Korsmeyer–Peppas Drug Release Kinetics Models

Table 1. Correlation Coefficients of Kinetics Models

Kinetics Model	Correlation Coefficient (R^2)		
	Al/HAp5	Al/HAp10	Al/HAp15
Zero-order	0.637	0.808	0.740
First-order	0.880	0.924	0.959
Higuchi	0.886	0.989	0.985
Hixson–Crowell	0.718	0.879	0.827
Korsmeyer–Peppas	0.916	0.972	0.972

The CDR of each sample was fitted to the zero-order, first-order, Higuchi, Hixson–Crowell, and Korsmeyer–Peppas kinetics models. The plots shown in Figure 5 were used to determine the behavior of acetaminophen release from the nanocomposite beads. The correlation coefficients obtained from the kinetics models are provided in Table 1. The correlation coefficient values indicated that the best correlation with all samples was shown by the Korsmeyer–Peppas model, wherein drug release occurred through quasi-Fickian diffusion from polymer matrices through the membrane to receptor mediaas illustrated by the release exponent (n) values of 0.199, 0.238, and 0.225 for Al/HAp5, Al/HAp10, and Al/HAp15, respectively [21]. The value of n describes the types of diffusion, wherein a value less than 0.45 corresponds to the Fickian diffusion mechanism, which is governed by the gradient of chemical potential or differences in concentrations [32]. The release of acetaminophen can be accompanied by minor swelling or friction inside the beads [33]. The release rate constant k was approximately 5.11, 4.69, and 4.93 for Al/HAp5, Al/HAp10, and Al/HAp15, respectively. The release rate constant showed a narrow range of values for all types of beads, with the increased loading of hydroxyapatite resulting in sustained drug release by reducing the release rate constant. Previous research on the utilization of inorganic materials used hydroxyapatite to administer acetaminophen and demonstrated that acetaminophen loading reached 48.5% and that most of the drug was released after 8 h [23]. The combination of organic and inorganic materials showed highly promising results. In a previous study, acetaminophen release can be sustained for up to 200 h by using glass–ceramic porous scaffolds coated with chitosan [34].

Conclusions

The alginate–hydroxyapatite samples were fairly capable of producing a steady increment in drug release rate with the increase in hydroxyapatite amount. The addition of hydroxyapatite could provide additional active sites in the beads that could help retain acetaminophen and prolong drug release. The release of acetaminophen from the solid matrices can be maintained for 48 h and was governed by the Fickian diffusion mechanism. Therefore, the combination of hydroxyapatite and alginate has potential applications in the biomedical field as a drug carrier medium to achieve a controlled drug delivery system.

Acknowledgments

We thank Chemical Engineering Department Universiti Teknologi PETRONAS for providing the facility and analysis to conduct the experiments.

References

[1] Adepu, S., Ramakrishna, S. 2021. Controlled Drug Delivery Systems: Current Status and Future Directions. Molecules. 26(19): 5905, https://doi.org/10.3390/molecules26195905.

[2] Ku, A., *et al*. 2019. Auger electrons for cancer therapy–a review. EJNMMI Radiopharm. Chem. 4(1): 27, https://doi.org/10.1186/s41181-019-0075-2.

[3] Chiew, A.L., *et al*. 2020. Hepatotoxicity in a child following an accidental overdose of liquid paracetamol. Clin. Toxicol. 58(11): 1063–1066, https://doi.org/ 10.1080/15563650.2020.1722150.

[4] Trucillo, P. 2021. Drug Carriers: Classification, Administration, Release Profiles, and Industrial Approach. Process. 9(3): 470, https://doi.org/10.3390/pr9030470.

[5] Lara-Ochoa, S., Ortega-Lara, W., Guerrero-Beltrán, C.E. 2021. Hydroxyapatite Nanoparticles in Drug Delivery: Physicochemistry and Applications. Pharm. 13(10): 1642, https://doi.org/10.3390/pharmaceutics13101642.

[6] Eskitoros-Togay, Ş.M., Bulbul, Y.E., Dilsizc, N. 2020. Dilsiz, Combination of nano-hydroxyapatite and curcumin in a biopolymer blend matrix: Characteristics and drug release performance of fibrous composite material systems. Int. J. Pharm. 590: 119933, https://doi.org/10.1016/j.ijpharm.2020.119933.

[7] Iravani, S., Soufi, G.J. 2021. Algae-derived materials for tissue engineering and regenerative

medicine applications: current trends and future perspectives. Emergent Mater. 5: 631–652, https://doi.org/ 10.1007/s42247-021-00283-6.

[8] Puscaselu, G.R., *et al*. 2020. Alginate: From Food Industry to Biomedical Applications and Management of Metabolic Disorders. Polym. 12(10): 2417, https://doi.org/10.3390/polym12102417.

[9] Jariya, S.A.I., *et al*. 2021. Drug delivery and antimicrobial studies of chitosan-alginate based hydroxyapatite bioscaffolds formed by the Casein micelle assisted synthesis. Mater. Chem. Phys. 272: 125019, https://doi.org/10.1016/j.matchemphys.2021.125019.

[10] Liu, S.-M., *et al*. 2021. In Vitro Evaluation of Calcium Phosphate Bone Cement Composite Hydrogel Beads of Cross-Linked Gelatin-Alginate with Gentamicin-Impregnated Porous Scaffold. Pharm. 14(10): 1000, https://doi.org/10.3390/ph14101000.

[11] Prakash, J., *et al*. 2019. PVA/alginate/hydroxyapatite films for controlled release of amoxicillin for the treatment of periodontal defects. Appl. Surf. Sci. 495: 143543, https://doi.org/10.1016/j.apsusc.2019.143543.

[12] Bi, Y.-g., Lin, Z.-t., Deng, S.-t. 2019. Fabrication and characterization of hydroxyapatite/sodium alginate/chitosan composite microspheres for drug delivery and bone tissue engineering. Mater. Sci. Eng. C. 100: 576–583, https://doi.org/10.1016/j.msec.2019.03.040.

[13] Nie, L., *et al*. 2021. Silver-doped biphasic calcium phosphate/alginate microclusters with antibacterial property and controlled doxorubicin delivery. J. Appl. Polym. Sci. 138(19): 50433, https://doi.org/10.1002/app.50433.

[14] Ren, B., *et al*. 2018. Injectable polysaccharide hydrogel embedded with hydroxyapatite and calcium carbonate for drug delivery and bone tissue engineering. Int. J. Biol. Macromol. 118: 1257–1266, https://doi.org/10.1016/j.ijbiomac.2018.06.200.

[15] Sukhodub, L.F., *et al*. 2018. Synthesis and characterization of hydroxyapatite-alginate nanostructured composites for the controlled drug release. Mater. Chem. Phys. 217: 228–234, https://doi.org/10.1016/j.matchemphys.2018.06.071.

[16] Rial, R., *et al*. 2021. The design and green nanofabrication of noble hydrogel systems with encapsulation of doped bioactive hydroxyapatite toward sustained drug delivery. J. Mol. Liq. 343: 117598, https://doi.org/10.1016/j.molliq.2021.117598.

[17] Yue, Y., Collaku, A., Liu, D.J. 2018. Evaluation of a 12-Hour Sustained-Release Acetaminophen (Paracetamol) Formulation: A Randomized, 3-Way Crossover Pharmacokinetic and Safety Study in Healthy Volunteers. Clin. Pharmacol. Drug Dev. 7(1): 95–101, https://doi.org/ 10.1002/cpdd.367.

[18] Benson, M., *et al*. 2009. Patient preference for sustained-release versus standard paracetamol (*acetaminophen*): a multicentre, randomized, open-label, two-way crossover study in subjects with knee osteoarthritis. J. Int. Med. Res. 37(5): 1321–1335, https://doi.org/ 10.1177/147323000903700507.

[19] Choi, G., *et al*. 2021. Inorganic–inorganic nanohybrids for drug delivery, imaging and photo-therapy: recent developments and future scope. Chem. Sci. 12(14): 5044–5063, https://doi.org/10.1039/D0SC06724E.

[20] Tan, I.K.G., *et al*. 2020. Composite of Kaolin/Sodium Alginate (SA) Beads for Methylene Blue Adsorption. ASEAN J. Chem. Eng. 19(2): 100, https://doi.org/ 10.22146/ajche.51457.

[21] Padmaa, P.M., *et al*. 2018. Release Kinetics-Concepts and Applications. Int. J. Pharm. Res. Technol. 8(1): 12, https://doi.org/10.31838/ijprt/08.01.02.

[22] DileepKumar, V.G., *et al*. 2022. A review on the synthesis and properties of hydroxyapatite for biomedical applications. J. Biomater. Sci. Polym. Ed. 33(2): 229–261. https://doi.org/10.1080/09205063.2021.1980985.

[23] Chung, H.K., *et al*. 2020. Biowaste-derived carbon dots/hydroxyapatite nanocomposite as drug delivery vehicle for acetaminophen. J. Sol-Gel Sci. Technol. 93(1): 214–223, https://doi.org/10.1007/s10971-019-05141-w.

[24] Zhang, J., Wang, Q., Wang, A. 2010. In situ generation of sodium alginate/hydroxyapatite nanocomposite beads as drug-controlled release matrices. Acta Biomaterialia. 6(2): 445–454, https://doi.org/10.1016/j.actbio.2009.07.001.

[25] Rincón-López, J.A., *et al*. 2018. Synthesis, Characterization and In Vitro Study of Synthetic and Bovine-Derived Hydroxyapatite Ceramics: A Comparison. Mater. 11(3): 333, https://doi.org/10.3390/ma11030333.

[26] Bajas, D., *et al*. 2021. Formulation and Characterization of Alginate-Based Membranes for the Potential Transdermal Delivery of Methotrexate. Polym. 13(1): 161, https://doi.org/10.3390/polym13010161.

[27] Dalal, S.R., *et al*. 2021. Characterization of alginate extracted from Sargassum latifolium and its use in Chlorella vulgaris growth promotion and riboflavin drug delivery. Sci. Rep. 11(1): 16741, https://doi.org/ 10.1038/s41598-021-96202-0.

[28] Derkach, S., *et al*. 2019. Interactions between gelatin and sodium alginate: UV and FTIR studies. J. Dispersion Sci. Technol. 41: 1–9, https://doi.org/ 10.1080/01932691.2019.1611437.

[29] Agougui, H., Guesmi, Y., Jabli, M. 2021. Preparation of Functionalized Hydroxyapatite with Biopolymers as Efficient Adsorbents of Methylene Blue. In Papadakis, R. (eds.), Dyes and Pigments -

Novel Applications and Waste Treatment, IntechOpen Limited. United Kingdom. pp. 327–385.
[30] Chen, S., *et al*. 2020. Biomimetic mineralization of nanocrystalline hydroxyapatites on aminated modified polylactic acid microspheres to develop a novel drug delivery system for alendronate. Mater. Sci. Eng. C. 110: 110655, https://doi.org/10.1016/ j.msec.2020.110655.
[31] Pradid, J., *et al*. 2017. Biological properties and enzymatic degradation studies of clindamycin-loaded PLA/HAp microspheres prepared from crocodile bones. Polym. Bull. 74(12): 5181–5194, https://doi.org/ 10.1007/s00289-017-2006-2.
[32] Amarachi, C.S., Onunkwo, G., Onyishi, I. 2013. Kinetics and mechanisms of drug release from swellable and non swellable matrices: A review. Res. J. Pharm. Biol. Chem. Sci. 4: 97–103.
[33] Moodley, T. and M. Singh, Polymeric Mesoporous Silica Nanoparticles for Enhanced Delivery of 5-Fluorouracil In Vitro. Pharmaceutics, 2019. 11(6): p. 288. https://doi.org/10.3390/pharmaceutics11060288.
[34] Villicaña-Molina, E., *et al*. 2019. Preparation of CEL2 glass-ceramic porous scaffolds coated with chitosan microspheres that have a drug delivery function. Int. J. Appl. Ceramic Technol. 16(5): 1812–1822, https://doi.org/10.1111/ijac.13196.